The 4q25 variant rs13143308T links risk of atrial fibrillation to defective calcium homeostasis

Adela Herraiz-Martínez[1,7], Anna Llach[2,7], Carmen Tarifa[1,7], Estefanía Lozano-Velasco[3], Selma A. Serra[1,7], Jorge Nicolas Domínguez[3], Jorge Gandía[1], Alexander Vallmitjana[4], Eduardo Vázquez Ruiz de Castroviejo[5], Raul Benítez[4], Amelia Aranega[3], Christian Muñoz-Guijosa[6], Diego Franco[3], Juan Cinca[2,7,8], Leif Hove-Madsen[1,7,8]

[1]Cardiovascular Research Centre CSIC; [2]Department of Cardiology, Hospital de la Santa Creu i Sant Pau, Barcelona, [3]Department of Experimental Biology, University of Jaén; [4]Department of Automatic Control, Universitat Politècnica de Catalunya, Barcelona; [5]Cardiology Unit, Regional Hospital Ciudad de Jáen; [6]Department of Cardiac Surgery, Hospital de la Santa Creu i Sant Pau; [7]IIB Sant Pau, Barcelona, Spain, [8]CIBERCV

Conflict of interests: The authors have declared that no conflict of interest exists

Correspondence:

Leif Hove-Madsen

Cardiac Rhythm and Contraction,

Centro de Investigación Cardiovascular CSIC,

Antiguo Hospital de la Santa Creu i Sant Pau, Pabellon 11

St Antoni Mª Claret 167, 08025 Barcelona, Spain

Phone: +34 935565620; Fax: +34 935565603

E-mail: lhove@csic-iccc.org

ABSTRACT

Single nucleotide polymorphisms on chromosome 4q25 have been associated with risk of atrial fibrillation (AF). However, the exiguous knowledge of the mechanistic links between these risk variants and underlying electrophysiological alterations hampers their clinical utility. Here, we used RT-PCR analysis, western blotting, confocal calcium imaging, and patch-clamp techniques to identify mechanisms linking 4q25 risk variants rs2200733T, rs13143308T or rs1448818G to defects in the calcium homeostasis observed in AF. Our findings revealed that the rs13143308T variant was more frequent in patients with AF and that it was associated with a significantly higher sarcoplasmic reticulum (SR) calcium ATPase expression, SR calcium load, calcium spark density and spontaneous electrical activity than the normal rs13143308G variant. Additionally, pitx2c expression was depressed in rs13143308T carriers, and a transgenic mouse model with atrial-specific heterozygous PITX2C deficiency faithfully reproduced the alterations in calcium homeostasis and electrical activity observed in rs13143308T carriers, supporting a regulatory role for pitx2c. Thus, we identify the 4q25 variant rs13143308T as a genetic risk marker for AF, specifically associated with excessive calcium release and spontaneous electrical activity caused by alterations in the expression and activity of SR calcium regulatory proteins, and possibly induced by deficient pitx2c expression in carriers of this risk variant.

Key words: Human atrial myocytes; Single nucleotide polymorphisms; Sarcoplasmic reticulum calcium release; Spontaneous electrical activity; pitx2c deficiency

INTRODUCTION:

Atrial fibrillation (AF) is the most common cardiac arrhythmia and a major contributory factor to increase mortality and risk of cerebrovascular embolism(1). Unfortunately, current treatments are often deficient or ineffective.

A number of electrophysiological, molecular, and structural alterations take place in the fibrillating atria that favor the maintenance and self-perpetuation of the arrhythmia(2, 3). Among the electrophysiological alterations, several studies have reported disturbances in the calcium homeostasis(4-7) and malfunctioning of the sarcoplasmic reticulum (SR)(4, 5, 7-10). Indeed, myocytes from patients with AF depict a high rate of spontaneous SR calcium release(4), which has been linked to deficient phosphodiesterase activity(11), reduced phosphatase activity(12), or excessive protein kinase A-(5, 9) or calmodulin kinase type II-dependent(8, 10, 13) phosphorylation of the cardiac ryanodine receptor (RyR2). Importantly, spontaneous calcium waves can induce arrhythmogenic membrane depolarizations in atrial myocytes from patients with AF(10), and occur both in resting and electrically stimulated human atrial myocytes(14, 15). Moreover, transgenic mouse models with high rates of spontaneous calcium release are more prone to present arrhythmia(10, 16-18); supporting the notion that spontaneous SR calcium release plays a central role in these arrhythmogenic processes.

Thus, electrophysiological mechanistic studies are narrowing down the molecular mechanisms that underlie defective calcium homeostasis in AF. Still, specific molecular triggers of AF are not well defined, except from mutations in ion channels associated to familial AF(19-21) that only account for a minority of the patients with AF. However, genome wide association studies have identified several single nucleotide polymorphisms (SNP)s on chromosomes 4q25, 1q21 and 16q22 that are associated with AF(22, 23) and recent meta-analyses have further expanded the number of risk variants(24). The most striking arrhythmogenic variants remain those located at 4q25(25) and some of them have been reported to modify the risk of AF recurrence after catheter ablation(26) and the response to

antiarrhythmic drug treatment(27). Furthermore, since the bicoid-related homedomain transcription factor Pitx2 plays a critical role in cardiac development, and is located in the vicinity of the 4q25 variants, Gudbjartsson et al.(22) postulated that Pitx2 dysfunction could be the molecular link between risk variants at 4q25 and AF. While studies have examined Pitx2 expression in patients with 4q25 risk variants(28, 29) and in patients with AF(29-31) the results from these studies are inconclusive regarding the link between 4q25 risk variants, Pitx2 function, and AF; thus hampering stratification and treatment based on the 4q25 genotype.

On the other hand, no studies have so far investigated if the 4q25 risk variants entail electrophysiological disturbances that are commonly associated to functional alterations in the intracellular calcium homeostasis. Therefore, we here tested the hypothesis that risk variants on chromosome 4q25 are genetic triggers of alterations in the intracellular calcium homeostasis reported in patients with AF.

RESULTS

4q25 risk variants in the study population

Genotyping was done in 543 patients for the 4q25 risk variants rs2200733T and rs13143308T that are highly associated with AF risk(22, 32) and subsequently in 253 patients for the rs1448818G risk variant that is closer to the PITX2 locus(33). The rs13143308T risk variant was more frequent in patients with AF (p=0.005) while risk variants rs2200733T and rs1448818G depicted non-significant trends (supplementary figure 1). The rs2200733T risk variant co-segregated with rs13143308T (p<0.001; supplementary figure 2A), whereas there was no significant co-segregation of rs2200733 with rs1448818 or rs13143308 with rs1448818 (supplementary figure 2B-C). Atrial tissue samples and/or myocytes from 280 of these patients were used for further genetic, electrophysiological and/or molecular biological analysis. The clinical and echocardiographic data as well as pharmacological treatments of these patients are summarized in Table 1.

Impact of the 4q25 risk variant rs13143308T on spontaneous electrical activity

Since the rs2200733 and rs13143308 variants have repeatedly been associated with increased risk of AF, our analysis initially focused on these variants. However, since the two variants are located next to each other[30] and the rs2200733T risk variant occurred together with the rs13143308T risk variant in myocytes isolated from all but one of the patients, the specific effect of the rs2200733T variant could not be measured directly. Therefore, analysis initially focused on how the rs13143308T risk variant affected calcium homeostasis. First, we analyzed the frequency of transient inward currents (I_{TI}) resulting from extrusion of spontaneously released calcium by the Na-Ca exchanger (NCX). In patients without AF, the I_{TI} frequency was significantly higher in myocytes from patients carrying the rs13143308T risk variant (Figure 1A-B) while the I_{TI}-amplitudes were similar for patients with and without risk alleles (Figure 1C). Current-clamp experiments, performed in myocytes from a subset of patients to determine the net impact of calcium release-induced Na^{+}-Ca^{2+} exchange on the membrane potential, showed a higher amplitude and frequency of spontaneous membrane

depolarizations in carriers of the risk variant (Figure 1D-F). In two of the patients with risk variants some of the membrane depolarizations were large enough to trigger spontaneous action potentials.

Impact of the 4q25 risk variant rs13143308T on calcium homeostasis

Using frame-scanning confocal calcium imaging to visualize local calcium release from RyR2 clusters (calcium sparks) in a longitudinal plane of the myocyte revealed that the spark frequency was significantly higher in patients carrying a rs13143308T risk variant than in those with normal variants at rs2200733 and rs13143308 (figure 2A-B). This was due to a higher density of spark sites (Figure 2C) rather than a higher firing frequency per site (Figure 2D). Analysis of the spark properties (figure 3A-B) showed that the 4q25 risk variants did not affect the spark amplitude (Figure 3C), duration (Figure 3D) or width (Figure 3E).

Immuofluorescent labeling of total and ser2808 phosphorylated RyR2 clusters revealed that the presence of a risk variant did not affect the density of RyR2 clusters (0.59±0.10 vs. 0.56±0.07 clusters/µm2) but it significantly increased the ser2808/RyR2 intensity ratio, suggesting that the rs13143308T variant favors RyR2 phoshporylation at ser2808 (Figure 4A). Measurements of the caffeine releasable SR calcium load from the time-integral of the caffeine induced NCX current were also significantly higher in atrial myocytes from patients with a 4q25 risk variant (Figure 4B), which could potentially increase the number of RyR2 clusters that reach the threshold for spontaneous calcium release and thereby the density of calcium spark sites. By contrast, plotting the NCX rate against the calcium available for extrusion by the NCX to assess the NCX activity (see supplementary figure 3 for details) showed no difference between the resulting slopes for patients with normal and risk variants (Figure 4C).

Western blot analysis of SR calcium regulatory proteins revealed that expression of the cardiac sarco-endoplasmatic reticulum calcium ATPase (SERCA2a) was significantly higher in patients with a rs13143308T risk variant (Figure 4D) while expression of the SR calcium buffering protein calsequestrin-2 (CSQ-2) and the NCX were similar in patients with and without risk variants.

Combined and independent effects of the rs13143308 risk variant and atrial fibrillation

To determine if the rs13143308T risk variant exacerbates calcium-handling disturbances in AF, we determined whether the presence of the risk variant and/or AF had independent effects on the calcium homeostasis using a linear regression model. Analysis of myocytes from 68 patients showed that both the rs13143308 genotype (p=0.004) and AF (p=0.005) independently increased the I_{TI} frequency. Comparison of specific patient groups showed that patients with No AF carrying a risk allele had a 5-fold higher I_{TI} frequency than those with No AF and normal alleles at rs2200733 and rs13143308 (table 2, p<0.001). On the other hand AF increased the I_{TI} frequency four-fold in patients with the normal allele (p=0.004). Moreover, the effects of AF and 4q25 risk variants were additive with the I_{TI} frequency being 2.3-fold higher in patients with AF and a risk variant than in patients with AF but with normal variants. Analysis of the caffeine induced NCX current in a subset of 53 patients revealed that the SR calcium load was significantly modified by the genotype (p=0.001) but not by AF (p=0.128). Comparison of patient groups revealed a significantly higher SR calcium load in patients without AF that carry the rs13143308T risk variant. There were no differences in SR calcium loading or in NCX-activity between patients with AF carrying normal or risk variants (table 2). Analysis of the L-type calcium current (I_{Ca}), which is strongly reduced in patients with AF, revealed that the risk variants had no effect on I_{Ca} amplitude or properties in patients with or without AF (supplementary figure 4).

Differential effects of different 4q25 risk variants on calcium homeostasis

To determine if different 4q25 risk variants have similar effects on calcium homeostasis, we used a linear regression model to determine the effects of the most common genotype combinations of risk variants at the rs2200733, rs13143308 and rs1448818 loci. Taking into account potentially confounding effects of AF, this analysis revealed that the I_{TI} frequency was not altered by the presence of a single risk variant at rs1448818. By contrast, the I_{TI} frequency was significantly higher in patients carrying a single risk variant at rs13143308 (p<0.001) or double risk at rs2200733 and rs13143308 (p<0.001, Figure 5A). Carriers of a single rs13143308 risk variant also had significantly higher SR calcium loading than patients with no risk or with a single rs1448818G risk allele (Figure

5B). Analysis of L-type calcium current (I_{Ca}), revealed no significant differences between the four most common genotypes (Figure 5C), suggesting that the 4q25 risk variants are not targeting the L-type calcium channel in the right atrium.

4q25 risk variants, pitx2c deficiency and calcium homeostasis

Analysis of the mRNA levels of pitx2c, which has been proposed to mediate the effect of 4q25 risk variants, showed that pitx2 levels were significantly reduced in samples from patients with a single risk variant at rs13143308 (p=0.03) as compared to pitx2c levels in samples from patients with a single risk variant at rs1448818 or in samples from patients without risk variants at any of the three loci analyzed (Figure 6A). Analysis of mRNA levels of key calcium regulatory proteins in the same samples showed higher atp2a2 levels and the atp2a2/pln ratio in samples with a single rs13143308T risk variant (supplementary figure 5), which may contribute to increase SR calcium loading in myocytes from patients with this genotype. No significant changes were observed in ryr2, pln, or ncx1 levels for any risk variant (supplementary figure 5).

Theoretically, the reduced pitx2c expression observed in our patients with the rs13143308T risk variant could underlie the changes in calcium homeostasis observed in patients with this variant. In support of this hypothesis, an atrial-specific conditional heterozygous mouse model of pitx2c insufficiency (in which pitx2 levels are reduced by 75% in heterozygotes(34) revealed that right atrial myocytes from $pitx2^{fl/-}$ mice faithfully reproduced all the effects of the rs13143308T risk variant in humans on spontaneous calcium release (figure 6B), calcium waves, I_{Tl} frequency, SR calcium load (supplementary Figure 6), and spontaneous electrical activity both at rest (Figure 6C-D) and during stimulation (Figure 6E). Afterdepolarizations were not observed at any stimulation frequency between 0.5 and 4 Hz in any of four $Pitx2^{fl/fl}$ mice.

Of notice, the calcium spark frequency was also 3.9 fold higher in 22 left atrial myocytes from 6 $Pitx2^{fl/-}$ mice than in 25 left atrial myocytes from 8 $Pitx2^{fl/fl}$ mice (52.7±9.2 vs. 13.5±3.5 sparks/min/1000μm^2; p<0.001), demonstrating that pitx2 deficiency promote spontaneous SR calcium release in both right and left atrial myocytes.

DISCUSSION

Main findings

This study is the first to show that human atrial myocytes from patients with the rs13143308T AF risk variant at chromosome 4q25 have deficient pitx2c expression and an abnormally high incidence of both calcium release-induced I_{TI} currents and spontaneous membrane depolarizations. Since these electrophysiological alterations are recognized hallmarks of AF(4, 10), the fact that we observe them even in patients without AF suggests that the rs13143308T variant is a genetic risk marker for AF that entails excessive spontaneous calcium release-induced electrical activity.

Mechanisms promoting spontaneous SR calcium release in the 4q25 risk variant rs13143308T

Confocal calcium imaging in human atrial myocytes from our patients revealed that the 4q25 risk variant rs13143308T promotes spontaneous calcium waves as a result of an increase in the number of calcium spark sites. Since calcium sparks are produced by opening of the RyR2, a high open probability of the RyR2 has been alluded to account for an increased incidence of spontaneous calcium sparks and waves (35, 36). Mechanistically, an increased RyR2 opening may result from several factors, such as luminal calcium activation(37-39), hyperphosphorylation of the RyR2(5, 8-10, 40), and/or increased SR calcium loading(7, 41). In accordance with this, we found higher RyR2 phosphorylation at ser2808, higher expression of the SR calcium pump protein (SERCA2), atp2a2 mRNA levels and the atp2a2/pln ratio, as well as higher SR calcium loading in carriers of the rs13143308T risk variant that were free of AF. These findings, combined with the lack of concurrent increase in the SR calcium buffering protein CSQ-2, suggest that a greater number of RyR2 could reach the threshold for spontaneous calcium release(42) and consequently, lead to an increased calcium spark frequency. Interestingly the increase in SR calcium loading was only observed in risk carriers free of AF. This suggests that the rs13143308T mediated increase in SR calcium loading may precede the occurrence of AF and might contribute to the initiation of the arrhythmia. In support of

this assumption, a higher SR calcium load has been found in patients with paroxysmal AF(7) but not in patients with permanent AF(4, 5, 7, 8, 10).

The 4q25 risk variant rs13143308T as a genetic risk marker of atrial fibrillation linked to spontaneous electrical activity

Analysis of specific 4q25 genotype combinations at the loci rs2200733, rs13143308 and rs1448818 revealed that the presence of a risk variant at rs1448818 coinciding with normal variants at the other loci did not modify the I_{TI} frequency. By contrast, a single risk allele at rs13143308 coinciding with normal variants at the other loci increased the I_{TI} frequency 5-fold. Assessment of the specific effect of the rs2200733T risk allele is complex because we found, as others(22), that rs2200733T co-segregates with rs13143308T. Thus, genotyping for the rs13143308 allele alone would be sufficient to identify patients at risk of AF associated with excessive spontaneous calcium release.

Functionally, the presence of a single rs13143308T risk variant increased both the frequency and amplitude of spontaneous membrane depolarizations (Figure 1D-F). Of notice, the amplitude of the I_{TI} was similar in patients with and without the risk variant (Figure 1A-C). Considering that the I_{TI} amplitude is expected to reflect electrogenic Na^{+}-Ca^{2+} exchange and hence determine the amplitude of the membrane depolarization, the above findings suggests that the larger depolarizations in patients with the rs13143308T variant might occur because the risk variant induce a concurrent reduction in repolarizing ionic currents, which would increase the depolarization produced by the I_{TI}. In support of this notion, patients with AF present a reduction in potassium currents in the right atrium that help repolarizing the myocyte and stabilize the resting membrane potential(43, 44). Thus, the present findings warrant future studies analyzing the effect of 4q25 risk variants on the expression and activity of potassium channels stabilizing the resting membrane potential.

A prominent reduction in the I_{Ca} density is another characteristic feature of atrial myocytes from patients with AF(5, 6, 31). However, none of the three risk variants examined here had any effect on the amplitude or properties of I_{Ca} in patients with or without AF; suggesting no role for L-type channels as a functional link between these 4q25 risk variants and AF.

Pitx2c as a molecular link promoting excessive calcium homeostasis and electrical activity in the rs13143308T risk variant

The transcription factor Pitx2c plays a pivotal role in cardiac development, regulating the expression of proteins such as connexins and ion channels(30) whose expression is altered in patients with AF; and it has been proposed as a molecular substrate linking 4q25 risk variants and atrial fibrillation(22). In agreement with previous studies, which failed to find effects of the rs2200733 or rs1448818 risk alleles on pitx2c levels(28, 29), we observed pitx2c levels in samples from patients with risk alleles at rs2200733 or rs1448818 that were similar to the pitx2c levels in patients without risk alleles at any of the three loci examined. However, the presence of a single rs13143308T risk variant was associated with a significant reduction in the pitx2c level (see figure 6A), which concurred with significant increases in SERCA2 (atp2a2) mRNA levels and the atp2a2/plb ratio, supporting the notion that alterations in the SR calcium homeostasis observed in patients with the rs13143308T risk variant could be regulated by pitx2c. Further support to this notion is provided by the results from a transgenic mouse model with conditional heterozygous atrial-specific pitx2c deletion, which faithfully reproduced all the effects of the rs13143308T variant on calcium homeostasis and spontaneous electrical activity in humans (see figure 6B-E and supplementary figure 6). Moreover, this model presents alterations in calcium regulatory proteins compatible with our findings in humans(34) and it displays features associated with AF such as atrial dilation, AV-nodal block, and missing p-waves(30).

Study limitations

Human right atrial samples. Due to ethical constrains, our study was limited to the use of human right atrial specimens because they can be routinely obtained at the time of right atrial cannulation during the majority of surgical cardiac interventions that use extracorporeal circulatory support. In contrast, tissue samples from the left atrium are only available in patients undergoing interventions that require opening of the left atrium, such as mitral valve surgery. Even in these cases, the left atrium is often dilated and affected structurally and this has been reported to disturb the calcium homeostasis(45). Therefore, an unbiased analysis of the calcium homeostasis and electrical activity is

feasible in human right atrial samples but much less so in left atrial samples. Thus, we cannot rule out that some of our findings are specific to the right atrium. Underlying cardiovascular disease or pharmacological treatments could also influence our results, but there were no significant differences in the incidence of concurrent diseases or in the drug prescription among patients with and without 4q25 risk variants (see Table 1).

Functional effect of Pitx2c in right atrial samples. It is generally acknowledged that pitx2c expression levels are low in the right atrium, reaching levels that approach the detection limit and can give rise to considerable variation in pitx2c levels(30). This in turn has raised doubts about the functional relevance of Pitx2c in the right atrium as compared to the left atrium where pitx2c levels are 100-1000 fold higher(28, 30). Moreover, several studies have failed to demonstrate consistent links between 4q25, pitx2c expression, and AF(28-31), even in left atrial samples. Our findings are subject to the same limitations and, even though the effect of the rs13143308T variant on pitx2c expression has not been examined previously, we cannot rule out that the observed depression of pitx2c levels for this variant and the concurrent changes in calcium regulatory proteins could be secondary to modulation of another transcription factor(46). On the other hand, atrial-specific Pitx2c deficiency in our transgenic mouse model has previously been reported to produce atrial dilation in both right and left atria(30). Furthermore, in the present study right atrial myocytes from the pitx2c$^{fl/-}$ mice faithfully reproduced observations in the human right atrial samples and pitx2c deficiency had very similar effects on the SR calcium homeostasis and spontaneous electrical activity in right and left atrial pitx2c$^{fl/-}$ myocytes, demonstrating that Pitx2c deficiency has functionally relevant effects on calcium homeostasis in the right atrium and that these are similar to the effects observed in the left atrium.

Clinical implications

Our study identifies the 4q25 rs13143308T risk allele as a genetic marker for AF risk linked to excessive calcium release and spontaneous electrical activity. Clinically, this should provide novel means for 1) Identification of patients with AF or at risk of it, in whom the arrhythmia is specifically

linked to defective calcium homeostasis and 2) Improvement of stratification and treatment of patients with AF. Specifically, the abnormally high incidence of calcium release observed in patients with the rs13143308T variant settles the bases for testing whether current or novel pharmacological therapies targeting SR calcium release are more efficient in preventing AF in patients with this variant than in patients with normal rs13143308G alleles.

Conclusions

In conclusion, our results identify the rs13143308T risk variant on chromosome 4q25 as potential biomarker for AF linked to arrhythmogenic calcium release and a new key to understand the complex molecular mechanisms that link AF to perturbations in the calcium homeostasis.

METHODS

Human biological samples, SNP genotyping, and atrial myocyte experimentation. A total of 543 blood samples were genotyped for the presence of the normal 4q25 variants rs2200733C, rs13143308G and rs1448818T or for the corresponding AF risk variants rs2200733T, rs13143308T and rs1448818G. Right atrial myocardial samples were collected from 280 genotyped patients undergoing cardiac surgery with extracorporeal circulation. Each patient gave written consent to obtain blood and tissue samples. The latter would otherwise have been discarded during the surgical intervention. The study was approved by the Ethics Committees of the Spanish National DNA Bank (BNADN, Salamanca), Hospital de la Santa Creu i Sant Pau (Barcelona) and of the University of Jaén; and the investigation conforms to the principles outlined in the Declaration of Helsinki.

Human atrial myocyte isolation. Samples were excised from the right atrial appendage of patients undergoing cardiac surgery with extracorporeal circulation (mostly bypass and/or valve replacements). Samples were stored immediately in cold oxygenated Tyrode solution and snap-frozen or used for myocyte isolation within 5-10 min after excision. For myocyte isolation, the sample was cut into small fragments and digested in a calcium-free Tyrode solution with 1.2mg/ml collagenase (Worthington type 2, 255 or 298 u/mg), 0.45 mg/ml proteinase (Sigma type XXIV, 11 u/mg solid), and 2 mg/ml bovine fatty acid-free albumin. After 30 minutes, cells were liberated from the tissue fragments in Ca^{2+}-free solution by gentle agitation with a Pasteur pipette. The remaining tissue was digested for 3x15 minutes in calcium free solution containing 0.7 mg/ml collagenase. Only elongated cells with clear cross striations and without abnormal granulation were used.

Clinical characterization and SNP Genotyping. Clinical information relevant to this study and included in table 1 was collected from the clinical records by a clinician. Medication refers to the patient medication prescribed before the surgical intervention. Patients without any incidents of atrial fibrillation (AF) in the clinical record were considered free of the arrhythmia. Patients were classified as having paroxysmal or chronic AF according to the information available in the clinical

record. Chronic AF included patients having persistent or long-term persistent AF. To reduce fractioning of the data, patients with paroxysmal and chronic AF were pooled into a single group of AF patients. This grouping was done because unpublished data from our laboratory and published data(7) show that spontaneous calcium release is already elevated in patients with paroxysmal AF.

SNP genotyping. Polymerase chain reaction amplification of the SNPs rs2200733, rs13143308 and rs1448818 were carried out using flanking oligonucleotides as outlined in Supplementary Table 1, followed by direct sequencing. Genomic DNA samples from 174 patients with AF and 369 patients with no reported episodes of AF were included and analyzed. Samples from the 174 patients with AF were collected as follows: 75 at the Spanish National DNA Bank (BNADN, Salamanca), 68 at the Cardiology Service at Hospital de la Santa Creu i Sant Pau, Barcelona, and 31 at the Cardiology Unit of the Hospital Regional Ciudad de Jaén. Samples from the 369 patients free of FA were obtained from the Spanish National DNA Bank (BNADN, Salamanca) in 157 cases and from Hospital de la Santa Creu i Sant Pau (Barcelona) in 212 cases. For all atrial samples used for electrophysiological and/or molecular biological studies, genotyping was done for batches of samples after experiments had been performed and analyzed.

Transgenic mouse model and myocyte isolation. The Pitx2 floxed and NppaCre transgenic mouse lines have been described previously(30, 34). Wild type Cre- controls (NppaCre-Pitx2fl/fl) and atrial-specific heterozygous (NppaCre+Pitx2fl/-) mice were used in this study. Cardiomyocytes were isolated from 3-6 months-old NppaCre-Pitx2fl/fl and NppaCre+Pitx2+/- mice(2). Briefly, mice were anesthetized (I.P. medetomidine 1 mg/kg and ketamine 75 mg/kg) and heparinized (I.P. 25 IU/ml). Twenty minutes later, after cervical dislocation, the heart was quickly excised and arrested in ice-cold Ca2+-free Tyrode solution. Hearts were then Langendorff perfused with an enzymatic solution (collagenase, proteinase and BSA) of Ca2+-free Tyrode during approximately 8 min. Afterwards, the right atrial chamber was dissected and cut into small pieces, washed twice in Ca^{2+}-free Tyrode solution by gentle agitation, and transferred back into a fresh enzymatic solution for approximately 8 min. This process was repeated several times until an adequate number of elongated atrial myocytes

with clear striations had been released. Subsequently cells were pooled, centrifuged for 5 min at 500 rpm, resuspended in Tyrode solution, and the [Ca2+] was gradually increased to 1 mM. The experimentation with mouse atrial myocytes conforms to the Guide for the Care and Use of Laboratory Animals, and was approved by the Bioethical Committee at Hospital de Santa Creu i Sant Pau.

Western blot and immunofluorescent labelling. Approximately 20 mg of right atrial sample was pulverized in liquid nitrogen and homogenized in 200 µl of ice-cold lysis buffer containing (in mM): 50 HEPES, 100 NaCl, 2.5 EGTA, 10 glycerol-2-phosphate 1 DTT supplemented with a cocktail of protease inhibitors (Roche) and with 0.1% (v/v) Tween 20 and 10% (v/v) glycerol at pH=7.4. Proteins were separated by SDS-PAGE (10% acrylamide:bisacrylamide) and electrotransferred onto Immobilon polyvinylidene diflouride membranes (Millipore). Membranes were incubated with primary and secondary antibodies diluted in 5% non-fat dry milk. Antibodies against SERCA2 (#9580, Cell Signaling Technology), CSQ-2 (ab3516, Abcam) and NCX1 (ab135735, Abcam) were used. Detection was performed using the appropriate horseradish peroxidase-labeled IgG and the SupersignalTM detection system (Supersignal West DuraTM, Pierce). Molecular-mass standards (Bioline) were used to estimate protein size and glyceraldehyde-3-phosphate dehydrogenase (GAPDH; MAB374, Millipore) was used as a loading control. Immunoblots were digitized (GS-800 Calibrated Densitometer; Bio-Rad) and analyzed with the Quantity One 4.6.3 software (Bio-Rad).

Isolated myocytes were fixed with paraformaldehyde 4% for 5 minutes at room temperature. Subsequently, cells were first incubated with PBS / Glycine 0.1 M during 10 minutes and then with PBS / Triton X-100 0.2% for at least 30 minutes to permeabilize the cells. Non-specific sites were blocked with PBS / Tween 20, 0.2% and Horse serum, 10% for 30 minutes. Myocytes were inmunofluorescently labeled with the primary antibodies mouse anti-RyR2 (C3-33 NR07, 1:1000; calbiochem) and rabbit anti-ser2808-P (1:600, A010-30, Badrilla). After labeling, cells were washed again and stored with PBS-Azide, 0.2 % at 4ºC until visualization. The secondary antibodies

AlexaFluor 488 anti-mouse and AlexaFluor 594 anti-rabbit were diluted 1:1000. Images were acquired with a confocal microscope (Leica AOBS SP5) using a 63x glycerol immersion objective.

mRNA extraction, reverse transcription and real time PCR. RNA was obtained from human atrial samples using RNeasy Mini kit (Qiagen) and the RNA was treated with DNase using Rnase-Free DNase Set (Qiagen). Subsequently, reverse transcription was carried out using 1 µg of RNA and QuantiTect Reverse Transcription kit (Qiagen), and 1 µL of the reverse transcriptase was used with SsoFast EvaGreeen Supermix (Bio-Rad) for real time PCR, which was done using a CFX384 system from Bio-Rad. Quantification of the PCR was done using the 2-ΔΔCt method as previously described(2).

The following primer sequences were used for Pitx2c:

Pitx2c: 5´CTTTCCGTCTCCGGACTTTT3´

5´CGCGACGCTCTACTAGTCCT3´

Pitx2c expression was normalized to PPIA GAPDH, or NKX2.5 using the following primer sequences:

PPIA: 5´TCGAGTTGTCCACAGTCAGC3´

5´TTCATCTGCACTGCCAAGAC3´

GAPDH: 5´AGCCACATCGCTCAGACACA3´

5´AACCATGTAGTTGAGGTCAAT3´

NKX2.5: 5´CTTCACCGGCCAAGTGTG3´

5´GCCTCTGTCTTCTCCAGCTC3´

Linear regression analysis revealed that Pitx2c expression levels were highly correlated for all combinations of primer pairs. GADPH vs. PPIA: R2=0,752, n=50 $p<0.001$; NKX2.5 vs. PPIA: R2=0.815, n=17, $p<0.001$; NKX2.5 vs GADPH: R2=0.815, n=17, $p<0.001$.

Patch-clamp technique. I_{Ca} was elicited by a 200 ms depolarization to 0 mV and spontaneous I_{TI} currents were measured at holding potentials of -80 or -50 mV using whole cell voltage-clamp in the perforated patch configuration with a HEKA EPC-10 amplifier (HEKA Elektronik Dr. Schultze, Lambrecht/Pfalz, Germany). Na-currents were eliminated by a 50 ms depolarization to -50 mV prior to activation of I_{Ca}. Series resistance compensation was not performed. Access resistance was 9±0.5 MΩ. The extracellular solution contained (in mM): NaCl 127, TEA 5, HEPES 10, $NaHCO_3$ 4, NaH_2PO_4 0.33, glucose 10, pyruvic acid 5, $CaCl_2$ 2, $MgCl_2$ 1.8, (pH = 7.4). The pipette solution contained (in mM): aspartic acid 109, CsCl 47, Mg_2ATP 3, $MgCl_2$ 1, Na2phosphocreatine 5, Li_2GTP 0.42, HEPES 10 (pH = 7.2 with CsOH) and 250 μg/ml amphotericin B. Experiments began when the series resistance did not decrease further, and cells were discarded if it was larger than 6 times the pipette resistance. The I_{Ca} amplitude was determined as the difference between the peak inward current and the current at the end of the depolarization, and the current-voltage relationship for I_{Ca} was obtained using test potentials between -40 and +50 mV. Voltage-dependent inactivation was determined using pre-pulses between -40 and 0 mV followed by a second 200 ms depolarization to +10 mV, and data were fit with Boltzmann equation to determine the voltage for half-maximal inactivation. The time constants for I_{Ca} inactivation were determined from a double exponential fit of the decaying phase of I_{Ca}.

The SR calcium load was determined from the charge carried by the current elicited by rapid exposure to 10 mM caffeine for 5 to 10 s. The charge was converted to amoles (10^{-18} mol) of calcium released from the SR, assuming a stoichiometry of $3Na^+$:$1Ca^{2+}$ for the NCX and normalized to the cell capacitance. Experimental protocols were linked and executed sequentially. Erroneous measurement(s) were eliminated, giving rise to variations in the total number of experiments for different currents. Most of these cases occurred because exposure of myocytes to caffeine produced sudden increases in the leakage current or irreversible cell contracture in some myocytes. Similarly, in myocytes used for current clamp experiments, the I_{TI} frequency, but not I_{Ca} was determined using the voltage-clamp configuration

Membrane potentials were measured in the current-clamp configuration using K^+-containing intra and extracellular media. The bath solution contained (in mM): NaCl 136, KCl 4, NaH_2PO_4 0.33, $NaHCO_3$ 4, $CaCl_2$ 2, $MgCl_2$ 1.6, HEPES 10, Glucose 5, pyruvic acid 5, (pH = 7.4). The pipette solution contained (in mM): aspartic acid 109, KCl 47, Mg_2ATP 3, $MgCl_2$ 1, Na_2phosphocreatine 5, Li_2GTP 0.42, HEPES 10 (pH = 7.2 with KOH) and 250 µg/ml amphotericin B. The holding current was varied in order to assess the amplitude and frequency of spontaneous membrane depolarizations at different resting membrane potentials. Results were pooled in 10 mV intervals: -80mV represents the mean of events recorded at potentials between -85 and -76mV; -70mV: the mean between -75 and -66 mV and -60mV: the mean between -65 and -56mV.

Confocal calcium imaging. To visualize changes in the intracellular calcium concentration, myocytes were loaded with 2.5 µM fluo-4 AM. Confocal calcium images (512x140 pixels) were recorded at 90 Hz, using a resonance-scanning confocal microscope with a 63x glycerol-immersion objective (Leica SP5 AOBS, Wetzlar, Germany). Fluo-4 was excited at 488 nm and emission was measured between 500 and 650nm with a Leica Hybrid Detector. Laser power was set to 20% of 100 mW and then attenuated to 4%. Experiments were performed at room temperature.

To detect calcium sparks, a wavelet-based detection method was applied to the normalized time-dependent fluorescence signal zi(t) at every pixel in order to detect candidates for Ca2+ release events. More specifically, Gaussian wavelet of order 2 with scales from 5 to 10 were used in order to enhance Ca^{2+} release events with a duration of 20 to 300 ms. Candidate event regions were detected by thresholding the wavelet signals at 3.5 σ. The noise variance of the wavelet signal σ was robustly estimated using the median absolute deviation of the fluorescence signal of a pixel at the center of the cell. Subsequently, spark candidates were filtered based on a relative intensity threshold of 0.4, a full duration at half maximum between 10 and 150 ms, a spark decay constant between 15 to 150 ms and a minimal R^2 for the exponential fit of the decay of 0.5. To eliminate sparks occurring within a calcium wave, events with an elevated baseline (1.5x or higher) were eliminated. The program allowed visual inspection of the calcium signal in consecutive images and the spatial location of each

detected spark was indicated in the corresponding images in order to manually validate or reject doubtful events. The program also allowed merging of consecutive recordings from the same cell. After supervised validation and merging, sparks that coincided spatially (within a radius of 2 µm) were pooled into a common spark site and calcium traces were generated for each spark site. Each spark was characterized by its amplitude, its duration characterized as the Full Duration at Half Maximum (FDHM) and its width characterized as the Full Width at Half Maximun (FWHM). The spark frequency was calculated as the number of sparks/cell/s or normalized to the cell area within the confocal plane and expressed as sparks/μm^2/s. Additionally, the number of spark sites were expressed as sites/cell or normalized to the cell area and given as sites/μm^2. The average spark frequency per site was given as sparks/site/s.

Statistics Electrophysiological and molecular biological analysis of human atrial samples was performed without knowledge about clinical data or genotypes and clinicians gathering the clinical data did not know the experimental results. Data sets were analyzed with SPSS statistical software. Unless otherwise stated, values were averaged for each patient. Mean values are indicated with horizontal bars in dot plots or given as mean±s.e.m. as indicated. Statistical significance was evaluated using Fisher's exact test for categorical data. Student's t-test was used for paired or unpaired comparisons, and ANOVA or a linear regression model was used for comparison of multiple effects as indicated. For the statistical analysis of the effects of the different genotypes containing the three SNPs, we used a linear regression model taking into account the effects of the different genotypes, the presence of AF, and whether the patients were undergoing mitral valve replacement. Based on the linear regression model, the effect of AF and the most common genotypes was estimated and given as mean±s.e.m. Statistically significant effects are indicated with p-values or *: $p<0.05$, **: $p<0.01$; ***: $p<0.001$.

Author contributions

Designing study: DF, LH-M

Acquiring data: AH, AL, CT, EL-V, SAS, JND, JG, EVRC, CMG, LH-M

Analyzing and interpreting data: AH, CT, AV, RB, AA, DF, JC, LH-M

Writing the manuscript: JC, LH-M

Acknowledgements

The collaboration of the Department of Cardiac Surgery at Hospital de la Santa Creu i Sant Pau is greatly appreciated.

Sources of funding This work was supported by multi-centric grants from Centro Nacional de Investigaciones Cardiovasculares, [CNIC-2009-08] to LH-M and to DF; grants from the Spanish Ministry of Economy and Competition [SAF2014-58286-C2-1-R] to LHM and [DPI2013-44584-R] to RB; and from the Spanish Ministry of Health and Consume, Instituto de Salud Carlos III, Red de Investigación Cardiovascular [RD12/0042/0002] to JC, and Fondo Europeo de Desarrollo Regional (FEDER).

REFERENCES

1. Camm, A.J., Lip, G.Y., De Caterina, R., Savelieva, I., Atar, D., Hohnloser, S.H., Hindricks, G., and Kirchhof, P. 2012. 2012 focused update of the ESC Guidelines for the management of atrial fibrillation: an update of the 2010 ESC Guidelines for the management of atrial fibrillation. Developed with the special contribution of the European Heart Rhythm Association. *Eur Heart J* 33:2719-2747.
2. Wijffels, M.C., Kirchhof, C.J., Dorland, R., and Allessie, M.A. 1995. Atrial fibrillation begets atrial fibrillation. A study in awake chronically instrumented goats. *Circulation* 92:1954-1968.
3. Wakili, R., Voigt, N., Kaab, S., Dobrev, D., and Nattel, S. 2011. Recent advances in the molecular pathophysiology of atrial fibrillation. *J Clin Invest* 121:2955-2968.
4. Hove-Madsen, L., Llach, A., Bayes-Genis, A., Roura, S., Rodriguez Font, E., Aris, A., and Cinca, J. 2004. Atrial fibrillation is associated with increased spontaneous calcium release from the sarcoplasmic reticulum in human atrial myocytes. *Circulation* 110:1358-1363.
5. Llach, A., Molina, C.E., Prat-Vidal, C., Fernandes, J., Casado, V., Ciruela, F., Lluis, C., Franco, R., Cinca, J., and Hove-Madsen, L. 2011. Abnormal calcium handling in atrial fibrillation is linked to up-regulation of adenosine A2A receptors. *Eur Heart J* 32:721-729.
6. Van Wagoner, D.R., Pond, A.L., Lamorgese, M., Rossie, S.S., McCarthy, P.M., and Nerbonne, J.M. 1999. Atrial L-type Ca2+ currents and human atrial fibrillation. *Circ Res* 85:428-436.

7. Voigt, N., Heijman, J., Wang, Q., Chiang, D.Y., Li, N., Karck, M., Wehrens, X.H., Nattel, S., and Dobrev, D. 2014. Cellular and molecular mechanisms of atrial arrhythmogenesis in patients with paroxysmal atrial fibrillation. *Circulation* 129:145-156.

8. Neef, S., Dybkova, N., Sossalla, S., Ort, K.R., Fluschnik, N., Neumann, K., Seipelt, R., Schondube, F.A., Hasenfuss, G., and Maier, L.S. 2010. CaMKII-dependent diastolic SR Ca2+ leak and elevated diastolic Ca2+ levels in right atrial myocardium of patients with atrial fibrillation. *Circ Res* 106:1134-1144.

9. Vest, J.A., Wehrens, X.H., Reiken, S.R., Lehnart, S.E., Dobrev, D., Chandra, P., Danilo, P., Ravens, U., Rosen, M.R., and Marks, A.R. 2005. Defective cardiac ryanodine receptor regulation during atrial fibrillation. *Circulation* 111:2025-2032.

10. Voigt, N., Li, N., Wang, Q., Wang, W., Trafford, A.W., Abu-Taha, I., Sun, Q., Wieland, T., Ravens, U., Nattel, S., et al. 2012. Enhanced sarcoplasmic reticulum Ca2+ leak and increased Na+-Ca2+ exchanger function underlie delayed afterdepolarizations in patients with chronic atrial fibrillation. *Circulation* 125:2059-2070.

11. Molina, C.E., Leroy, J., Richter, W., Xie, M., Scheitrum, C., Lee, I.O., Maack, C., Rucker-Martin, C., Donzeau-Gouge, P., Verde, I., et al. 2012. Cyclic adenosine monophosphate phosphodiesterase type 4 protects against atrial arrhythmias. *J Am Coll Cardiol* 59:2182-2190.

12. El-Armouche, A., Boknik, P., Eschenhagen, T., Carrier, L., Knaut, M., Ravens, U., and Dobrev, D. 2006. Molecular determinants of altered Ca2+ handling in human chronic atrial fibrillation. *Circulation* 114:670-680.

13. Chelu, M.G., Sarma, S., Sood, S., Wang, S., van Oort, R.J., Skapura, D.G., Li, N., Santonastasi, M., Muller, F.U., Schmitz, W., et al. 2009. Calmodulin kinase II-

mediated sarcoplasmic reticulum Ca2+ leak promotes atrial fibrillation in mice. *J Clin Invest* 119:1940-1951.

14. Llach, A., Molina, C.E., Fernandes, J., Padro, J., Cinca, J., and Hove-Madsen, L. 2011. Sarcoplasmic reticulum and L-type Ca2+ channel activity regulate the beat-to-beat stability of calcium handling in human atrial myocytes. *J Physiol*.

15. Molina, C.E., Llach, A., Herraiz-Martinez, A., Tarifa, C., Barriga, M., Wiegerinck, R.F., Fernandes, J., Cabello, N., Vallmitjana, A., Benitez, R., et al. 2016. Prevention of adenosine A2A receptor activation diminishes beat-to-beat alternation in human atrial myocytes. *Basic Res Cardiol* 111:5.

16. Bai, Y., Jones, P.P., Guo, J., Zhong, X., Clark, R.B., Zhou, Q., Wang, R., Vallmitjana, A., Benitez, R., Hove-Madsen, L., et al. 2013. Phospholamban knockout breaks arrhythmogenic Ca(2)(+) waves and suppresses catecholaminergic polymorphic ventricular tachycardia in mice. *Circ Res* 113:517-526.

17. Hwang, H.S., Hasdemir, C., Laver, D., Mehra, D., Turhan, K., Faggioni, M., Yin, H., and Knollmann, B.C. 2011. Inhibition of Cardiac Ca2+ Release Channels (RyR2) Determines Efficacy of Class I Antiarrhythmic Drugs in Catecholaminergic Polymorphic Ventricular Tachycardia. *Circ Arrhythm Electrophysiol* 4:128-135.

18. Li, N., Chiang, D.Y., Wang, S., Wang, Q., Sun, L., Voigt, N., Respress, J.L., Ather, S., Skapura, D.G., Jordan, V.K., et al. 2014. Ryanodine receptor-mediated calcium leak drives progressive development of an atrial fibrillation substrate in a transgenic mouse model. *Circulation* 129:1276-1285.

19. Mahida, S., Lubitz, S.A., Rienstra, M., Milan, D.J., and Ellinor, P.T. 2011. Monogenic atrial fibrillation as pathophysiological paradigms. *Cardiovasc Res* 89:692-700.

20. Lubitz, S.A., Yin, X., Fontes, J.D., Magnani, J.W., Rienstra, M., Pai, M., Villalon, M.L., Vasan, R.S., Pencina, M.J., Levy, D., et al. 2010. Association between familial atrial fibrillation and risk of new-onset atrial fibrillation. *JAMA* 304:2263-2269.

21. Sabeh, M.K., and MacRae, C.A. 2010. The genetics of atrial fibrillation. *Curr Opin Cardiol* 25:186-191.

22. Gudbjartsson, D.F., Arnar, D.O., Helgadottir, A., Gretarsdottir, S., Holm, H., Sigurdsson, A., Jonasdottir, A., Baker, A., Thorleifsson, G., Kristjansson, K., et al. 2007. Variants conferring risk of atrial fibrillation on chromosome 4q25. *Nature* 448:353-357.

23. Liu, X., Wang, F., Knight, A.C., Zhao, J., and Xiao, J. 2012. Common variants for atrial fibrillation: results from genome-wide association studies. *Hum Genet* 131:33-39.

24. Sinner, M.F., Ellinor, P.T., Meitinger, T., Benjamin, E.J., and Kaab, S. 2011. Genome-wide association studies of atrial fibrillation: past, present, and future. *Cardiovasc Res* 89:701-709.

25. Ellinor, P.T., Lunetta, K.L., Albert, C.M., Glazer, N.L., Ritchie, M.D., Smith, A.V., Arking, D.E., Muller-Nurasyid, M., Krijthe, B.P., Lubitz, S.A., et al. 2012. Meta-analysis identifies six new susceptibility loci for atrial fibrillation. *Nat Genet* 44:670-675.

26. Husser, D., Adams, V., Piorkowski, C., Hindricks, G., and Bollmann, A. 2010. Chromosome 4q25 variants and atrial fibrillation recurrence after catheter ablation. *J Am Coll Cardiol* 55:747-753.

27. Parvez, B., Vaglio, J., Rowan, S., Muhammad, R., Kucera, G., Stubblefield, T., Carter, S., Roden, D., and Darbar, D. 2012. Symptomatic response to antiarrhythmic drug therapy is modulated by a common single nucleotide polymorphism in atrial fibrillation. *J Am Coll Cardiol* 60:539-545.

28. Gore-Panter, S.R., Hsu, J., Hanna, P., Gillinov, A.M., Pettersson, G., Newton, D.W., Moravec, C.S., Van Wagoner, D.R., Chung, M.K., Barnard, J., et al. 2014. Atrial Fibrillation associated chromosome 4q25 variants are not associated with PITX2c expression in human adult left atrial appendages. *PLoS One* 9:e86245.

29. Syeda, F., Holmes, A.P., Yu, T.Y., Tull, S., Kuhlmann, S.M., Pavlovic, D., Betney, D., Riley, G., Kucera, J.P., Jousset, F., et al. 2016. PITX2 Modulates Atrial Membrane Potential and the Antiarrhythmic Effects of Sodium-Channel Blockers. *J Am Coll Cardiol* 68:1881-1894.

30. Chinchilla, A., Daimi, H., Lozano-Velasco, E., Dominguez, J.N., Caballero, R., Delpon, E., Tamargo, J., Cinca, J., Hove-Madsen, L., Aranega, A.E., et al. 2011. PITX2 insufficiency leads to atrial electrical and structural remodeling linked to arrhythmogenesis. *Circ Cardiovasc Genet* 4:269-279.

31. Perez-Hernandez, M., Matamoros, M., Barana, A., Amoros, I., Gomez, R., Nunez, M., Sacristan, S., Pinto, A., Fernandez-Aviles, F., Tamargo, J., et al. 2016. Pitx2c increases in atrial myocytes from chronic atrial fibrillation patients enhancing IKs and decreasing ICa,L. *Cardiovasc Res* 109:431-441.

32. Lubitz, S.A., Sinner, M.F., Lunetta, K.L., Makino, S., Pfeufer, A., Rahman, R., Veltman, C.E., Barnard, J., Bis, J.C., Danik, S.P., et al. 2010. Independent susceptibility markers for atrial fibrillation on chromosome 4q25. *Circulation* 122:976-984.

33. Lubitz, S.A., Lunetta, K.L., Lin, H., Arking, D.E., Trompet, S., Li, G., Krijthe, B.P., Chasman, D.I., Barnard, J., Kleber, M.E., et al. 2014. Novel genetic markers associate with atrial fibrillation risk in Europeans and Japanese. *J Am Coll Cardiol* 63:1200-1210.

34. Lozano-Velasco, E., Hernandez-Torres, F., Daimi, H., Serra, S.A., Herraiz, A., Hove-Madsen, L., Aranega, A., and Franco, D. 2016. Pitx2 impairs calcium handling in a dose-dependent manner by modulating Wnt signalling. *Cardiovasc Res* 109:55-66.

35. Jiang, D., Xiao, B., Yang, D., Wang, R., Choi, P., Zhang, L., Cheng, H., and Chen, S.R. 2004. RyR2 mutations linked to ventricular tachycardia and sudden death reduce the threshold for store-overload-induced Ca2+ release (SOICR). *Proc Natl Acad Sci U S A* 101:13062-13067.

36. Jiang, D., Xiao, B., Zhang, L., and Chen, S.R. 2002. Enhanced basal activity of a cardiac Ca2+ release channel (ryanodine receptor) mutant associated with ventricular tachycardia and sudden death. *Circ Res* 91:218-225.

37. Lukyanenko, V., Viatchenko-Karpinski, S., Smirnov, A., Wiesner, T.F., and Gyorke, S. 2001. Dynamic regulation of sarcoplasmic reticulum Ca(2+) content and release by luminal Ca(2+)-sensitive leak in rat ventricular myocytes. *Biophys J* 81:785-798.

38. Jiang, D., Chen, W., Wang, R., Zhang, L., and Chen, S.R. 2007. Loss of luminal Ca2+ activation in the cardiac ryanodine receptor is associated with ventricular fibrillation and sudden death. *Proc Natl Acad Sci U S A* 104:18309-18314.

39. Jiang, D., Wang, R., Xiao, B., Kong, H., Hunt, D.J., Choi, P., Zhang, L., and Chen, S.R. 2005. Enhanced store overload-induced Ca2+ release and channel sensitivity to luminal Ca2+ activation are common defects of RyR2 mutations linked to ventricular tachycardia and sudden death. *Circ Res* 97:1173-1181.

40. Reiken, S., Wehrens, X.H., Vest, J.A., Barbone, A., Klotz, S., Mancini, D., Burkhoff, D., and Marks, A.R. 2003. Beta-blockers restore calcium release channel function and improve cardiac muscle performance in human heart failure. *Circulation* 107:2459-2466.

41. Diaz, M.E., O'Neill, S.C., and Eisner, D.A. 2004. Sarcoplasmic reticulum calcium content fluctuation is the key to cardiac alternans. *Circ Res* 94:650-656.

42. Viatchenko-Karpinski, S., Terentyev, D., Gyorke, I., Terentyeva, R., Volpe, P., Priori, S.G., Napolitano, C., Nori, A., Williams, S.C., and Gyorke, S. 2004. Abnormal calcium signaling and sudden cardiac death associated with mutation of calsequestrin. *Circ Res* 94:471-477.

43. Dobrev, D., Graf, E., Wettwer, E., Himmel, H.M., Hala, O., Doerfel, C., Christ, T., Schuler, S., and Ravens, U. 2001. Molecular basis of downregulation of G-protein-coupled inward rectifying K(+) current (I(K,ACh) in chronic human atrial fibrillation: decrease in GIRK4 mRNA correlates with reduced I(K,ACh) and muscarinic receptor-mediated shortening of action potentials. *Circulation* 104:2551-2557.

44. Van Wagoner, D.R., Pond, A.L., McCarthy, P.M., Trimmer, J.S., and Nerbonne, J.M. 1997. Outward K+ current densities and Kv1.5 expression are reduced in chronic human atrial fibrillation. *Circ Res* 80:772-781.

45. Dinanian, S., Boixel, C., Juin, C., Hulot, J.S., Coulombe, A., Rucker-Martin, C., Bonnet, N., Le Grand, B., Slama, M., Mercadier, J.J., et al. 2008. Downregulation of the calcium current in human right atrial myocytes from patients in sinus rhythm but with a high risk of atrial fibrillation. *Eur Heart J* 29:1190-1197.

46. Nadadur, R.D., Broman, M.T., Boukens, B., Mazurek, S.R., Yang, X., van den Boogaard, M., Bekeny, J., Gadek, M., Ward, T., Zhang, M., et al. 2016. Pitx2 modulates a Tbx5-dependent gene regulatory network to maintain atrial rhythm. *Sci Transl Med* 8:354ra115.

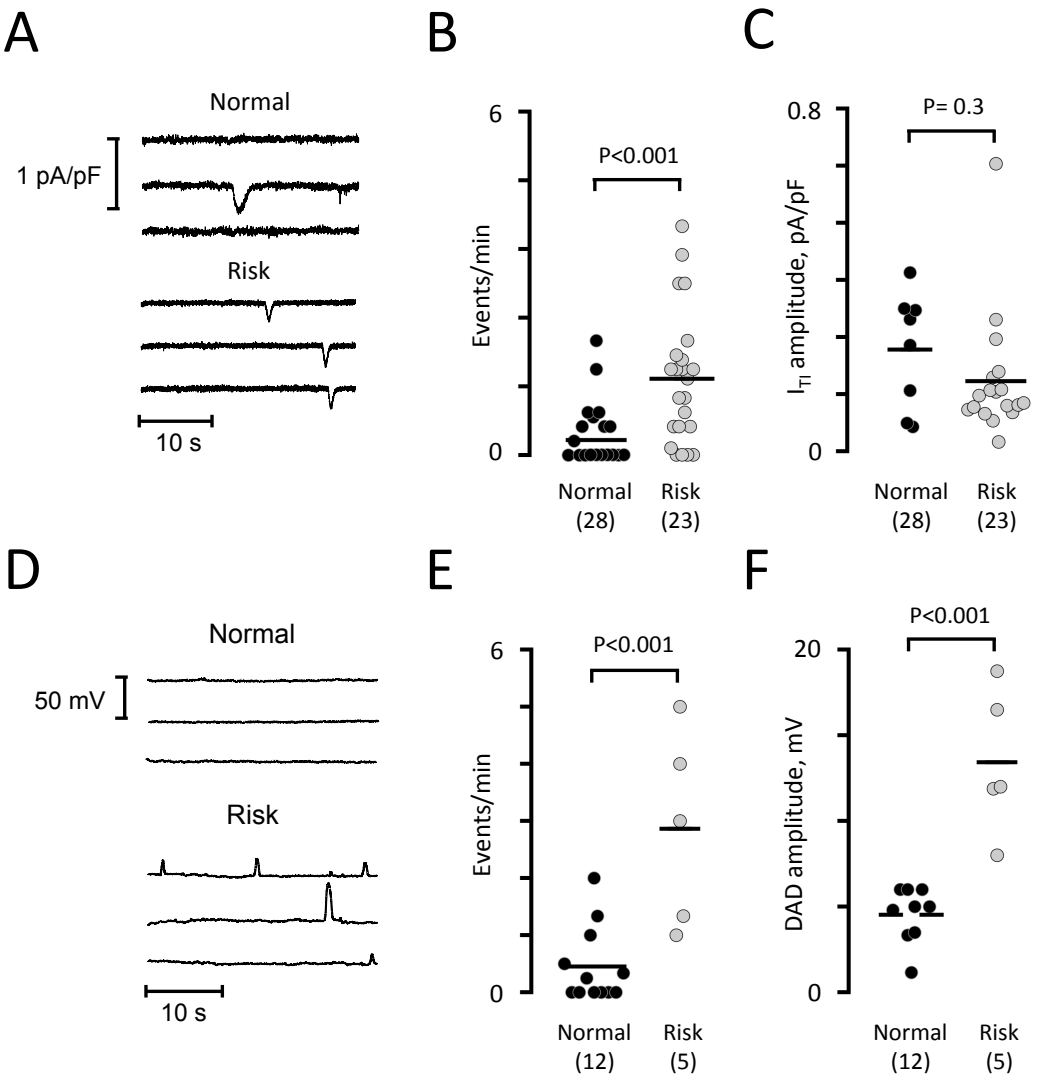

Figure 1. The risk variant rs13143308T increases spontaneous electrical activity.
A Spontaneous I_{TI} currents in patients with a normal or a risk variant at rs13143308. **B** I_{TI} frequency in myocytes with (risk) or without a risk variant (normal). **C** I_{TI} amplitude in the myocytes from panel B. **D** Membrane potential recordings at -80 mV in myocytes from a patient with normal and one with a risk variant. **E** Frequency of spontaneous membrane depolarizations at -80 mV in patients with normal and risk variants. **F** Amplitude of the depolarizations in the myocytes from panel E. P-values from unpaired t-tests are given above and the number of patients in parentheses.

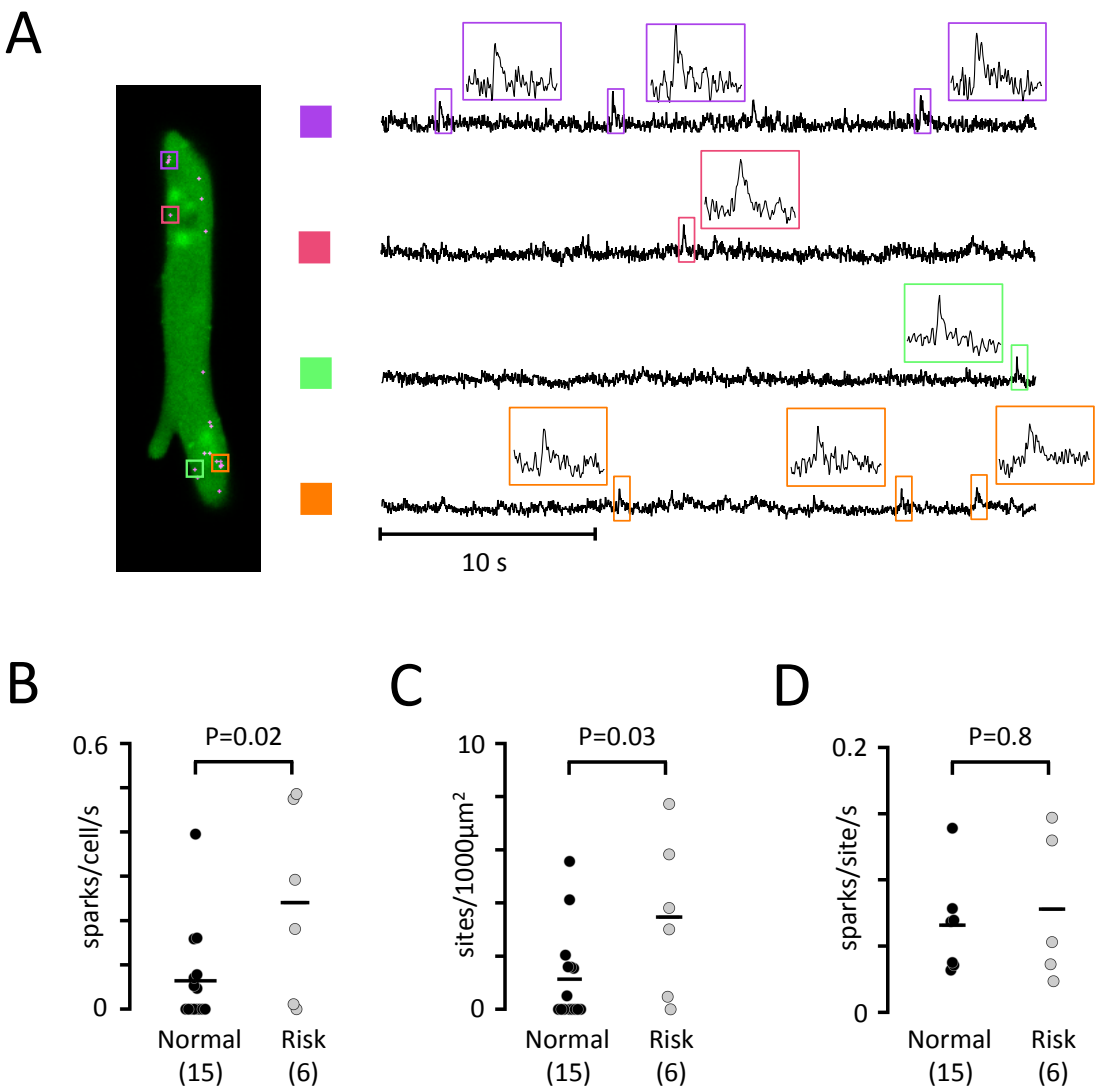

Figure 2. The rs13143308T risk variant increases the calcium spark density.
A Longitudinal plane of a human atrial myocyte from a patient with a 4q25 risk variant, with indication of four spark sites on the left (colored rectangles). Calcium signals are shown for each spark site on the right. Insets show calcium signals for individual sparks. **B** Spark frequency. **C** Spark sites per cell. **D** Spark firing frequency. P-values from unpaired t-tests are given above and the number of patients in parentheses.

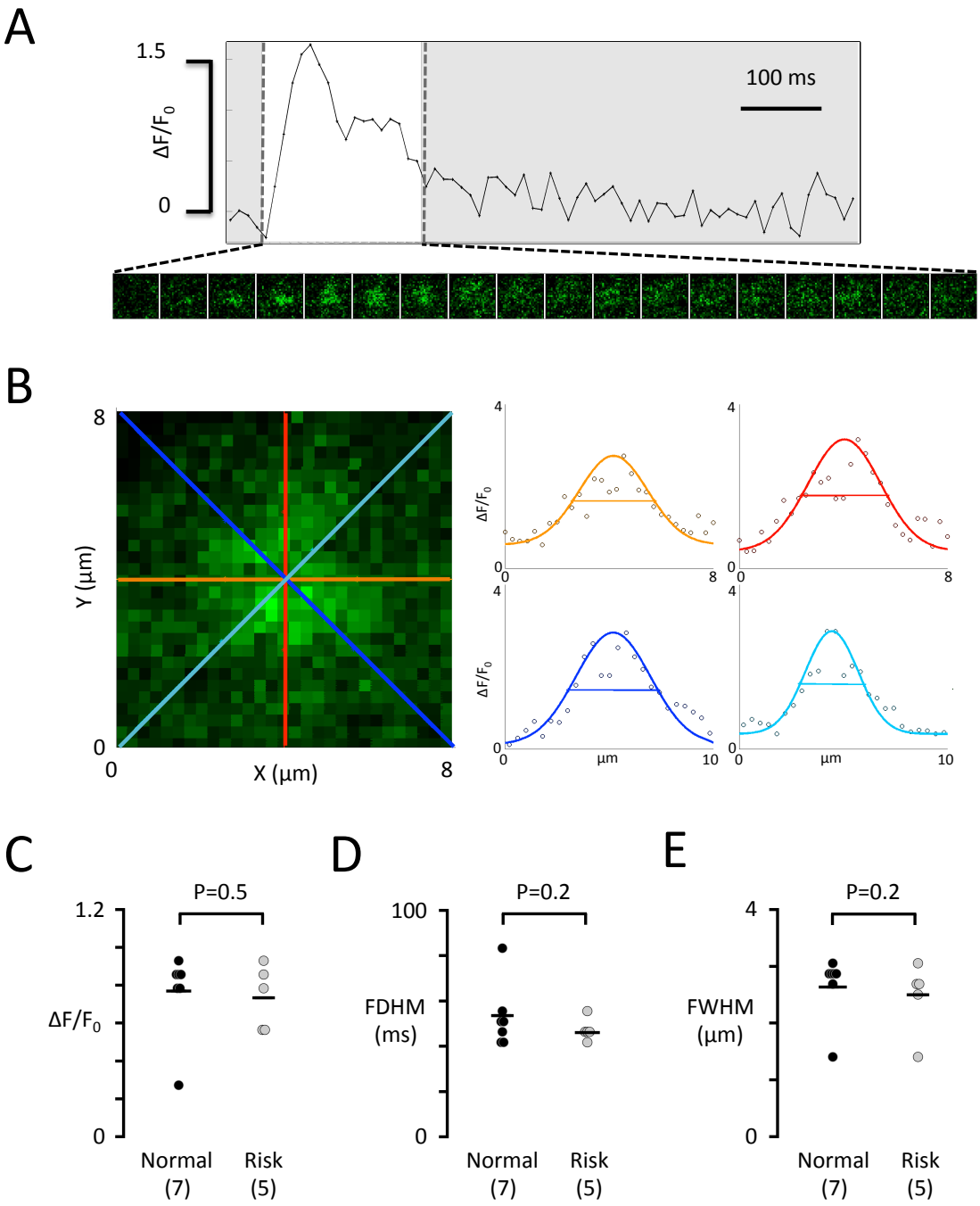

Figure 3. Calcium spark properties do not depend on the genotype at rs13143308.
A Ca^{2+} transient from a single spark site. Consecutive 8 x 8 µm images of the calcium spark are shown below the Ca^{2+} transient during its rise and decay (white window area). **B** Enlarged image of the calcium spark in panel A, recorded at its maximal amplitude. The profile of the calcium spark is shown on the right for each of the four colored axes outlined in the image on the left. The width of the calcium spark at half maximum (FWHM) was calculated as the average FWHM of the four axes **C** Calcium spark amplitude. **D** Calcium spark duration at half maximum (FDHM). **E** FWHM. Values are from the same myocytes as in figure 2. P-values for unpaired t-tests are given above and the number of patients is given in parentheses.

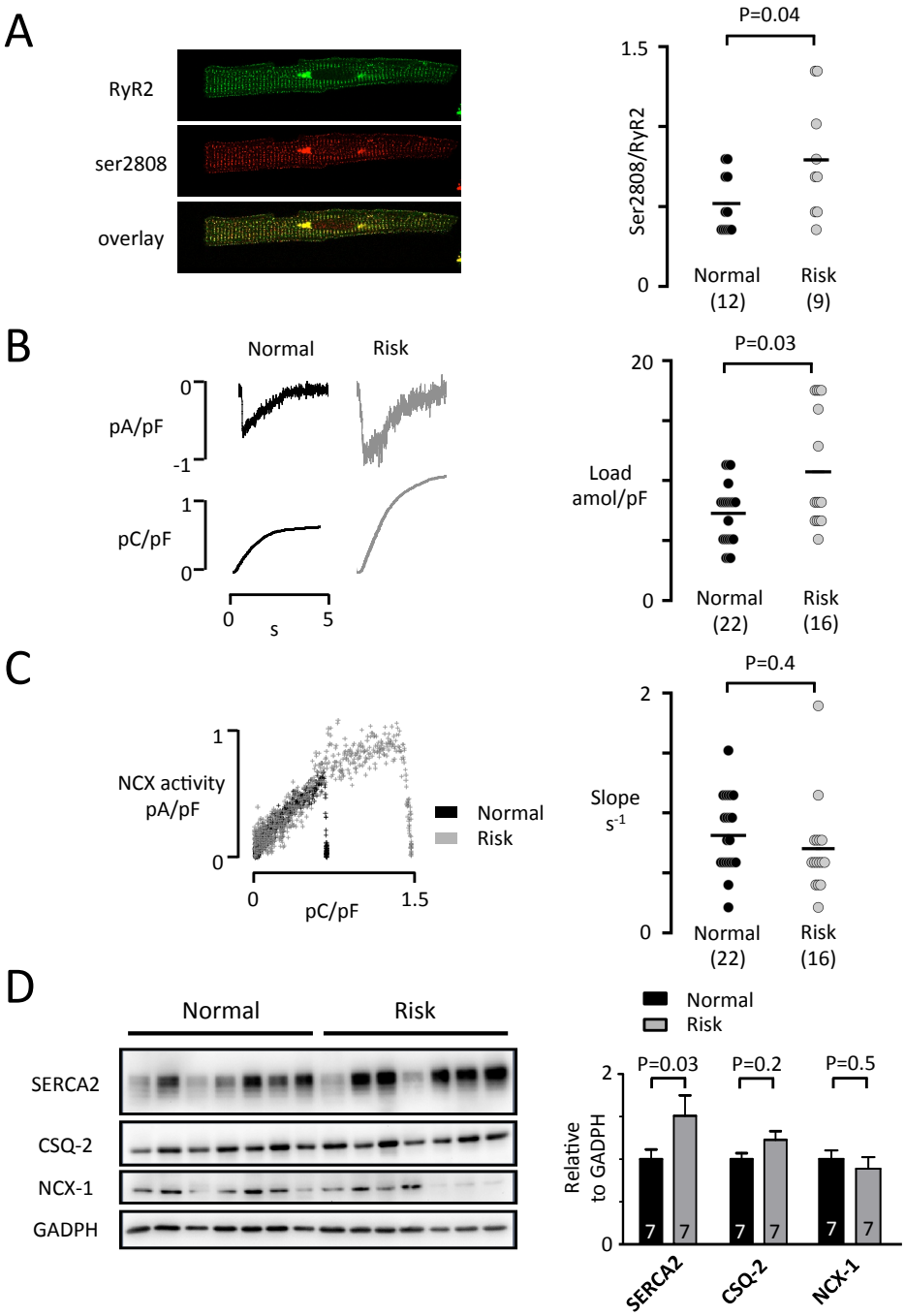

Figure 4. SR calcium loading and SERCA2 expression is increased in patients with the rs13143308T risk variant.

A Visualization of total RyR2 clusters (green) and ser2808 phosphorylated clusters (red) in a human atrial myocyte. The degree of ser2808 phosphorylation was estimated as the ratio of the ser2808/RyR2 intensity for each RyR2 cluster (right). **B** Caffeine-induced currents (top) and their time integral (bottom) for a normal and a risk variant. The SR calcium load is shown on the right. **C** Left: Relationship between the activity of the NCX and the calcium available for extrusion for a normal and a risk variant. The slopes of the relationships are shown on the right. **D** Immunoblots of SERCA2, CSQ-2, NCX-1 and GADPH in right atrial samples from patients with normal or risk variants at 4q25. GADPH served as reference. Mean SERCA2, CSQ-2 and NCX-1 expression levels are shown on the right. Values were normalized to the mean expression level in the normal variant. P-values for unpaired t-tests are given above and the number of patients is given in parentheses or on bars.

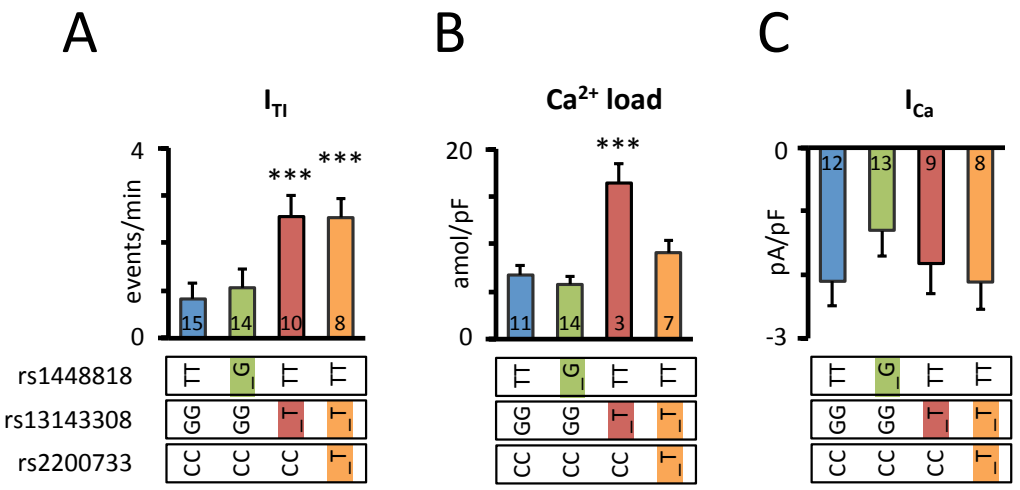

Figure 5. Effects of different 4q25 risk variants on calcium homeostasis.
A I_{TI} frequency in the four common combination of 4q25 polymorphisms at rs2200733, rs13143308 and rs1448818 indicated below bars. **B** Corresponding effects of these genotypes on SR calcium load. **C** Effect of the same genotypes on I_{Ca} amplitude. The number of patients is given for each bar. Statistical significance was determined using a linear regression model taking into account the genotype of all samples analyzed. *:p<0.05; **:p<0.01; ***:p<0.001.

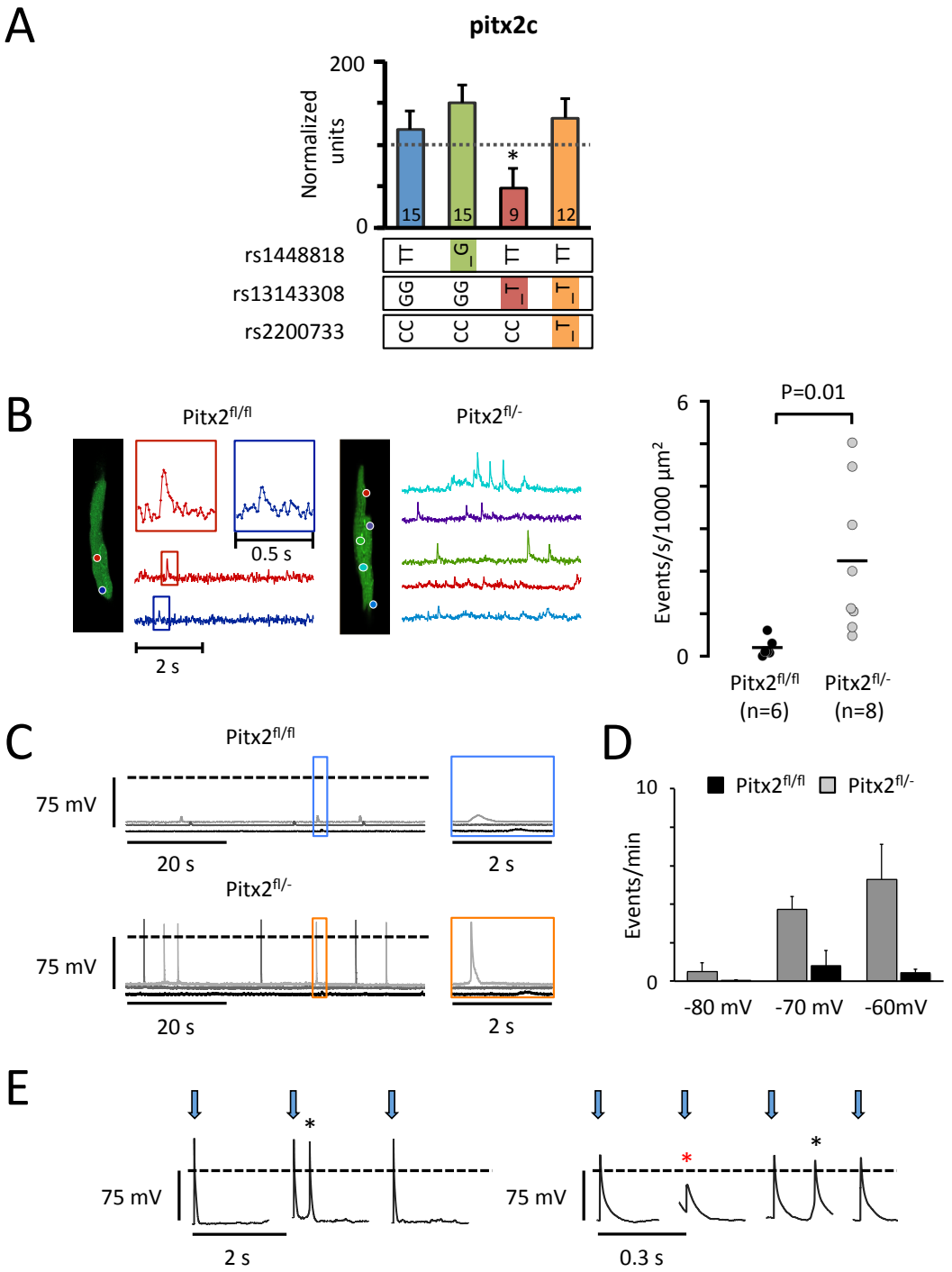

Figure 6. 4q25 risk variants, Pitx2 deficiency and calcium homeostasis.
A Pitx2c levels in the common combinations of the 4q25 variants rs2200733, rs13143308 and rs1448818, indicated below bars **B** Right atrial myocytes from a Pitx2$^{fl/fl}$ and a Pitx2$^{fl/-}$ mouse with indication of spark sites. Calcium traces from each site are shown to the right. Insets show details of the calcium sparks. Spark densities are shown on the right (unpaired t-test). **C** Membrane potential recordings in Pitx2$^{fl/fl}$ (top) and Pitx2$^{fl/-}$ mice (bottom). Traces are amplified on the right. **D** Frequency of spontaneous action potentials (events·min^{-1}) at resting potentials given below bars (8 Pitx2$^{fl/-}$ and 8 Pitx2$^{fl/fl}$ mice). Pitx2 deficiency significantly affected the spontaneous AP-frecuency ($p<0.05$, ANOVA). **E** Afterdepolarizations (black asterisks) in myocytes from Pitx2$^{fl/-}$ mice paced at 0.5 Hz (left) and 3 Hz (right). The red asterisk indicates an action potential diminished by a preceding afterdepolarization. Arrows indicate stimulation pulses and dashed lines 0 mV.

	Normal n=174	Risk n=106	p-value
Age (years)	68.0±0.8	66.7±0.8	0.8
Height (cm)	164.2±0.9	164.2±0.7	0.9
Weight (kg)	76±1	75±1	0.6
Cardiovascular disease % (n)			
Arterial hypertension	67 (117)	74 (78)	0.2
Diabetes	40 (69)	30 (32)	0.12
Aortic valve disease	49 (85)	57 (60)	0.2
Mitral valve disease	26 (45)	22 (23)	0.5
Tricuspid valve disease	13 (23)	9 (10)	0.4
Ischaemic heart disease	62 (108)	53 (56)	0.14
Echocardiography			
Left atrial diameter (mm)	46.6±1.0	44.6±1.2	0.2
Left atrial diameter index	2.61±0.07	2.47±0.08	0.2
LVEF (%)	55.2±1.1	58.0±1.3	0.11
Pharmacological treatment % (n)			
ACE-inhibitors	41 (72)	35 (38)	0.4
ARB	20 (34)	21 (23)	0.8
β-Blockers	52 (90)	56 (59)	0.4
Calcium antagonists	21 (38)	25 (27)	0.6
Nitrates	25 (44)	25 (26)	1
Dicoumarin	20 (35)	29 (31)	0.08
Acetyl salicylic acid	41 (72)	43 (46)	0.8
Statins	60 (105)	68 (72)	0.3

TABLE 1. Clinical characterization of the patients included in electrophysiological and molecular biological analyses. LVEF, left ventricular ejection fraction; ACE-inhibitors, angiotensin converting enzyme inhibitors; ARB angiotensin receptor blockers; Values are mean ± standard deviation or percentage and number (n) of patients with the condition. P-values for differences between Normal and Risk groups are given on the right.

	I_{TI}			Load			NCX		
4q25:	**Normal**	**Risk**	P	**Normal**	**Risk**	P	**Normal**	**Risk**	P
No AF (n)	0.26±0.09 (28)	1.33±0.24 (23)	0.001	7.28±0.54 (22)	10.16±1.36 (16)	0.03	0.81±0.07 (22)	0.70±0.10 (16)	0.37
AF (n)	1.04±0.32 (10)	2.44±0.83 (7)	0.09	6.93±0.77 (9)	5.20±0.64 (6)	0.09	0.86±0.09 (8)	1.00±0.25 (6)	0.49
P	0.004	0.09		0.72	0.19		0.73	0.22	

Table 2. Effect of rs13143308 variants on I_{TI} frequency, SR calcium Load, and NCX activity in patients without (No AF) and with AF. The I_{TI} frequency is given in events/min, the SR calcium load in amol/pF, and the NCX activity in s^{-1}. P-values for comparison of Normal and Risk variants are given in columns to the right of each comparison. Risk refers to the presence of at least one rs13143308T risk allele. Normal refers to patients with normal rs2200733C and rs13143308G alleles. P-values for comparison of No AF and AF are given below.